From *Light Metals 1986*, R.E. Miller, Editor

CORROSION AND PASSIVATION OF CERMET INERT ANODES
IN CRYOLITE-TYPE ELECTROLYTES

Gary P. Tarcy
Aluminum Company of America
Smelting Process Development Division
Alcoa Laboratories
Alcoa Center, PA 15069

Cermets are a class of materials that offer promise as inert anodes in aluminum smelting because of the low solubilities of certain oxides in cryolite and high conductivities of the metal phase. Electrochemical dissolution of the metal phase in the cermets can lead to premature failure of the anode. The electrochemical corrosion of various metals and alloy candidate phases has been investigated with linear sweep voltammetry, galvanostatic polarizations and microprobe elemental dot map analysis. The investigation showed that nickel is an unacceptable metal for cermet anodes. Noble metals are cathodically protected from anodic dissolution while copper/nickel alloys undergo a passivation. The passivation is strictly valid with cermets only and dependent on the use of copper rich alloys and high alumina concentrations in the melt. The passivation is independent of microstructural size of the alloy particles, concentration of the alloy phase, current density, dissolved aluminum metal and time.

INTRODUCTION

The concept of using inert anodes in the electrowinning of aluminum is as old as the Hall-Heroult process. Hall's original patents refer to the use of platinum and copper as non-consumable anodes. Although Hall recognized the possible advantages of inert anodes and spent considerable effort in their development, an acceptable inert anode material eluded the inventor. On January 20, 1911, in an address to the American Chemical Society, the American Electrochemical Society, and the Society of Chemical Industry, Hall said his work on inert anodes "delayed a successful result (other improvements in the overall smelting process) for a year or two."

An inert anode for aluminum smelting has continued to remain elusive. The most recent work on inert anodes has concentrated on two classes of materials, ceramic oxides and metals (1). The ceramic oxides had low solubility in molten cryolite but generally possessed poor electrical conductivity. This low conductivity dictated thin electrodes, which required extremely low corrosion rates. On the other hand, the metal electrodes had excellent electrical conductivity. However, except for the noble metals (e.g., Pt), the metal anodes were unstable with respect to oxygen. The oxide layers that formed also tended to spall. Neither the ceramic electrodes nor metal electrodes proved satisfactory as inert anodes.

Ray (2) introduced the concept of a cermet inert anode containing approximately 70% $NiFe_2O_4$/NiO

ceramic and 30% Ni metal. The nickel metal was intertwined throughout the ceramic base as a so-called wormy structure. The $NiFe_2O_4$/NiO had low chemical solubility in cryolite, imparting a high degree of dimensional stability to the anode. The nickel metal provided high electrical conductivity (300 ohm^{-1} cm^{-1}) and improved mechanical properties such as resistance to thermal shock.

Conceptually this cermet solved several problems of past materials. The cermet was highly conductive and fairly inexpensive; therefore, an anode having a thickness of several inches with a long but finite life was acceptable. In practice, several problems remained, the most significant being that the corrosion rate of the metal phase greatly exceeded the corrosion rate of the ceramic oxide phases. This paper describes an electrochemical study of the corrosion of the Ni metal phase in the $NiFe_2O_4$/NiO-Ni metal cermet. The corrosion study led to an experimental testing procedure and the development of an improved metal phase for the cermet. This testing procedure and improved metal phase cermet are also described in this paper.

EXPERIMENTAL

Two different cell designs were used to test the stability of various alloy phases in cermet inert anodes. One cell was used for corrosion studies and rapid screening of candidate materials. The second cell was used for longer term, more rigorous evaluation of the most promising material.

The cell shown in Figure 1 was used for the electrochemical corrosion studies and for screening various metals, alloys and cermets as inert anodes for aluminum smelting. The cell was a conventional three electrode design (3). The use of a molybdenum counter electrode was necessary to prevent interference of the corrosion current measurements caused by dissolved aluminum. The reference electrode was of traditional design (4). In order to define the electrode area, the working electrode was shielded with an alumina tube and immersed a minimum amount (<1 mm) into the electrolyte. A three-hour galvanostatic (1 amp/cm^2) polarization of the cermets or a half-hour galvanostatic (1 amp/cm^2) polarization of the metals was followed by a linear sweep voltammogram at 1 mv/sec. The open circuit potential (O.C.P.) was defined as the potential at which there was no current. The corrosion current was defined as the amount of anodic current that occurred on the

anode at a potential that was just cathodic of the thermodynamic oxygen evolution potential. After electrolysis, the anode was cross-sectioned and examined by electron microprobe analysis. The suitability of the material as an inert anode was judged by three criteria: low corrosion current, noble open circuit potentials, and microstructural integrity of the anode's metal phase.
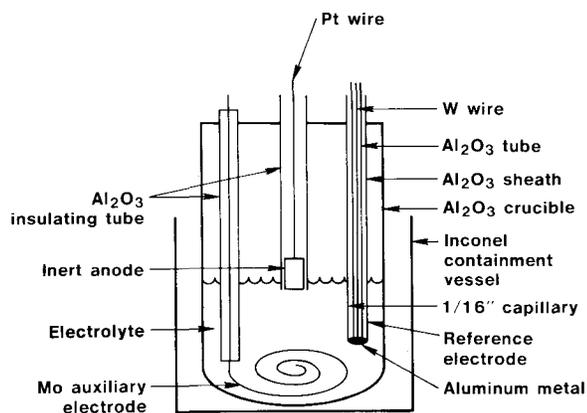

Figure 1. Cell design for electrochemical corrosion study and material screening.

The most promising anode material was galvanostatically polarized (1 amp/cm^2) for 100, 165 and 264 hours in three separate experiments. The extended time testing of the material was performed in a cell as shown in Figure 2. In the extended testing, it was necessary to simulate a conventional Hall cell. This required the use of carbon cathode bottom, insulating side walls (simulated with alumina liners), liquid aluminum metal cathodes, alumina feeding, and metal tapping. The condition of the metal phase in the anode after electrolysis was evaluated by cross-sectioning the anode and examining the integrity of the metal phase near the surface of the anode.

The instrumentation used in these studies is all commercially available. The voltammetry and three hour galvonastatic polarizations were performed with an EG&G Model 173 or Tacusell Model PIT 20-6X potentiostat. The potential or current was controlled with an EG&G Model 175 programmer. The ohmic losses were measured with an Electrosynthesis Company Model 800 IR measurement system. During the long term electrolysis experiments, the anode was galvanostaticly polarized with a Sorenson DCR 20-125 DC power supply.

The electrolyte composition was checked by analysis both before and after the experiment. Unless otherwise noted, all experiments in the short-term electrolysis cell (Figure 1) were carried out in a 1.15 NaF/AlF3 weight ratio, 5 wt% CaF2, saturated Al2O3 melt at 980°C.

All experiments in the long-term electrolysis cell (Figure 2) had the same electrolyte composition targets but operated at 960°C. Except for Al2O3 which was held at saturation by feeding at a rate consistent with 100% current efficiency, the target electrolyte composition varied considerably during the long-term electrolysis. No important impact on the anode was observed for the variations in melt composition.
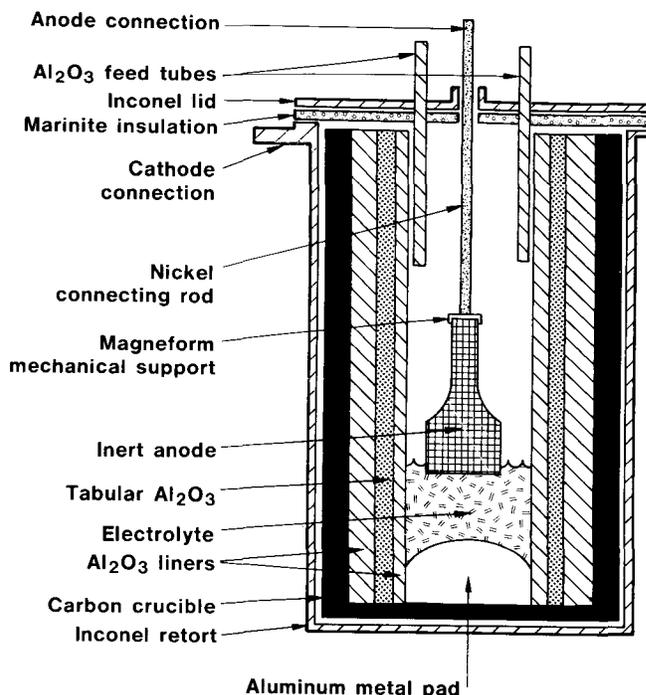

Figure 2. Cell design for extended time testing of inert anodes.

The cermet materials were fabricated by either reaction sintering or by conventional sintering. In the reaction sintering technique, the starting materials react during the sintering process to produce new phases (e.g., $5NiO + Fe_2O_3 + 2Fe \rightarrow 2NiFe_2O_4 + 3Ni$). In the conventional sintering technique, the starting materials are simply fused into the desired finished shape. In both cases the experimental fabrication procedures were the same: the starting materials were uniaxially or isostatically pressed at 20,000 psi and then sintered for two hours at 1350°C in an argon atmosphere.

The finished anode compositions are described below. The reaction sintered nickel metal cermet was a composite material containing nickel metal (actually 95% Ni, 5% Fe) as intertwined "worms" through the ceramic. The chemical composition was approximately 30% Ni, 56% $NiFe_2O_4$, and 14% NiO. The copper rich copper-nickel alloy cermet was a composite material having isolated metal particles in the ceramic base. Its chemical composition was 20% copper-nickel alloy (80% Cu, 20% Ni), 64% $NiFe_2O_4$, and 16% NiO. The platinum metal cermet also had isolated metal particles; the chemical composition was 20% Pt, 64% $NiFe_2O_4$, and 16% NiO. An isolated nickel metal cermet was also produced. The chemical composition was 20% Ni, 64% $NiFe_2O_4$, and 16% NiO. A reaction sintered interwoven copper-nickel alloy phase cermet was also made. The chemical composition was approximately 30% interwoven copper-nickel alloy (90% Ni:10% Cu), 56% $NiFe_2O_4$, and 14% NiO.

RESULTS AND DISCUSSION

Electrochemical Corrosion Study

During the development of Alcoa's inert anode, the most promising early candidate material was a reaction sintered $NiFe_2O_4$/NiO-Ni metal cermet material (2). The $NiFe_2O_4$ and NiO imparted a high degree of dimensional stability to the anode because of the low solubilities of these oxide phases in cryolite base electrolytes (5). The nickel metal in the anode provided high electrical conductivity and good mechanical strength.

Preferential corrosion of the alloy phase in this material was a problem. Figure 3 shows a photograph of a cross-sectioned anode after 96 hours of electrolysis. The darker region is the zone in which the metal has been leached from the material. This region had poor electrical conductivity (0.5 ohm^{-1} cm^{-1}) compared to the starting material (300 ohm^{-1} cm^{-1}) and lower mechanical strength. Microscopic examination of this region after the electrolysis period revealed two important differences from the unaffected region. First, the metal phase was completely missing. Second, the anode was much more porous and the pores were filled with frozen electrolyte.
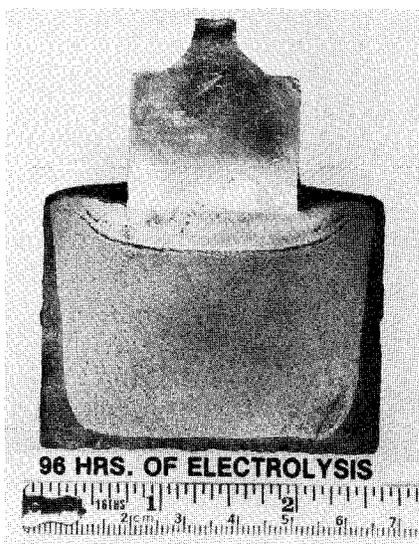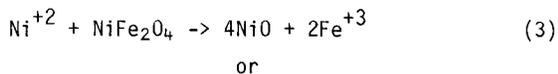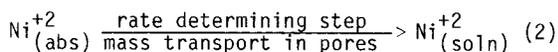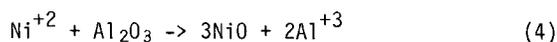

96 HRS. OF ELECTROLYSIS

Figure 3. Cross-section of a $NiFe_2O_4$/NiO-Ni metal inert anode.

The cause for this preferential corrosion has been identified as anodic dissolution of the nickel metal in the anode. Equations 1-6 below describe the anodic dissolution process.
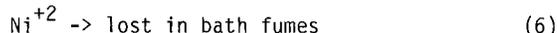
$$Ni = Ni^{+2} \text{ (abs)} + 2e \qquad (1)$$

$$Ni^{+2}_{\text{(abs)}} \xrightarrow{\text{rate determining step}}_{\text{mass transport in pores}} Ni^{+2}_{\text{(soln)}} \qquad (2)$$

$$Ni^{+2} + NiFe_2O_4 \rightarrow 4NiO + 2Fe^{+3} \qquad (3)$$

or

$$Ni^{+2} + Al_2O_3 \rightarrow 3NiO + 2Al^{+3} \qquad (4)$$

or

$$Ni^{+2} + 2e \rightarrow Ni \text{ (reduced into Al metal)} \qquad (5)$$

or

$$Ni^{+2} \rightarrow \text{lost in bath fumes} \qquad (6)$$

The primary anode reaction with inert anodes in aluminum smelting is oxygen evolution.

$$Al_2O_3 \rightarrow 2Al + 3/2\ O_2 \quad E^{\circ}_{980^{\circ}C} = 2.195 \text{ volts}$$
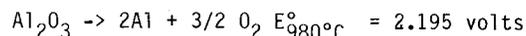
The anodic dissolution process manifests itself as an anodic corrosion current at potentials cathodic to the oxygen evolution potential. Figure 4 shows linear sweep voltammograms obtained using the $NiFe_2O_4$/NiO-Ni alloy cermet working electrode, and a platinum metal working electrode. An anodic current cathodic to the thermodynamic oxygen evolution potential is observed on the cermet anode, while it is absent on the platinum anode. In order to minimize the effect of uncontrolled variables (e.g., electrolyte impurities), both electrodes were of identical geometric size, and the experiment was performed on both materials with the same electrolyte in the same cell on the same day. Since no current below O_2 evolution was observed on the platinum anode, the current observed on the cermet anode was not the result of electrolyte impurities (e.g., dissolved Al or Na metal).
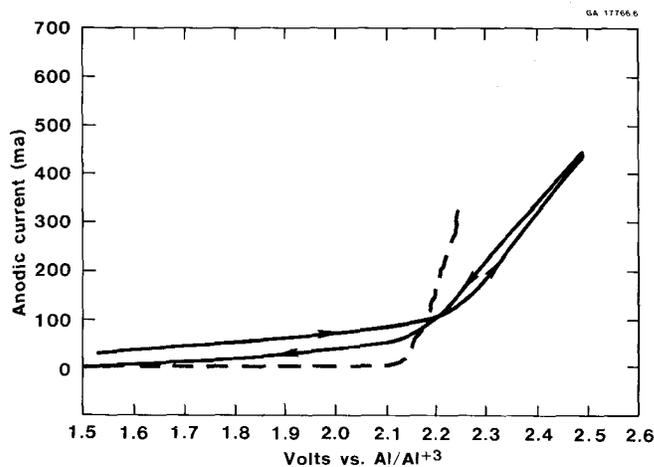

Figure 4. Linear sweep voltammograms of $NiFe_2O_4$/NiO-Ni cermet (—) and Pt (--) working electrodes (not I*R corrected).

The remote possibility that the corrosion current was caused by an underpotential evolution of oxygen was eliminated when no oxygen could be detected in the cell off-gas during polarization of the anode in the corrosion current region (2.0 volts vs Al).

This corrosion current is specific to the nickel metal alloy phase of the cermet. Figure 5 shows the linear sweep voltammograms obtained using a $NiFe_2O_4$/NiO-Ni cermet anode and a $NiFe_2O_4$/NiO ceramic anode. On the ceramic electrode, the only Faradaic process observed is oxygen evolution, while the cermet electrode exhibits two Faradaic processes. Oxygen

evolution is observed at potentials anodic to 2.2
volts. Anodic dissolution of the metal phase is
observed at potentials cathodic to 2.2 volts. Since
the corrosion current was eliminated by removing the
nickel metal from the anode, it is clear that this
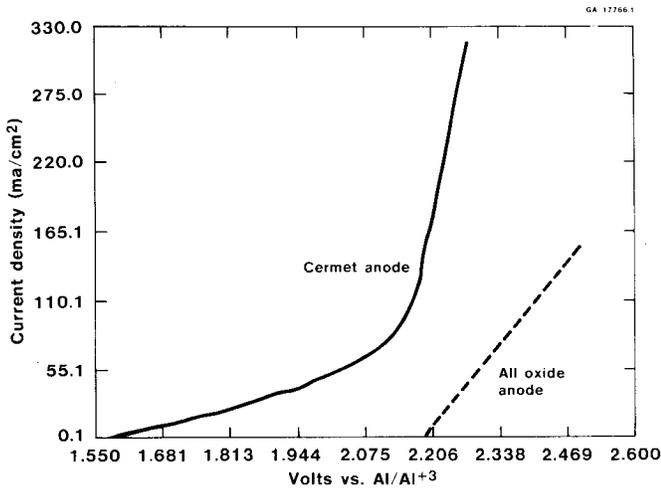corrosion current is caused by the nickel metal.

Figure 5. Linear sweep voltammograms of $NiFe_2O_4/$
$NiO-Ni$ cermet and $NiFe_2O_4/NiO$ ceramic anodes (not I*R
corrected).

A linear sweep voltammogram of the cermet anode
is plotted in a tafel format in Figure 6. A limiting
current was observed for the corrosion current indi-
cating that the process was mass transport con-
trolled. The limiting corrosion current decreased
slowly with time until a steady-state was achieved.
The steady-state limiting corrosion current density
varied from one anode to another, but was on the
average 26 ma/cm^2. The limiting corrosion current
density was also found to be independent of bulk
electrolyte mixing, indicating that mass transport
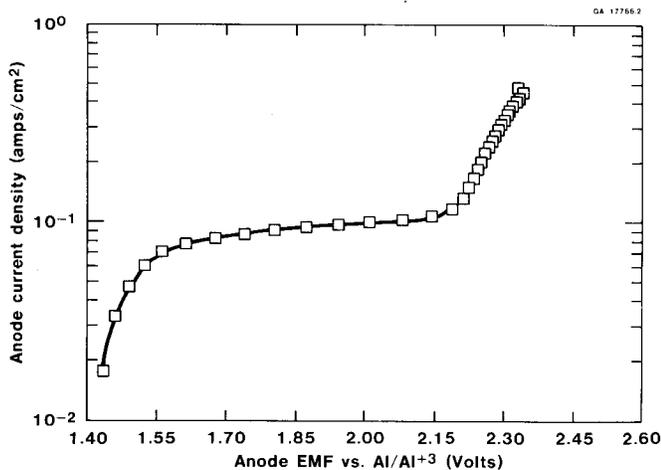control was occurring in the pores of the anode.

Figure 6. Voltammogram plotted in a Tafel format for
$NiFe_2O_4/NiO-Ni$ cermet.

Porous Electrode Discussion

A rigorous mathematical model for this cermet
electrode seemed unlikely. Compared to a smooth
electrode, any porous electrode is inherently com-
plicated by unequal electrochemical access. This
porous electrode was further complicated by a
changing pore structure. This dynamic pore structure
was the result of several processes. The primary
electrochemical process occurring in the pores
(anodic dissolution of Ni metal) was the primary pore
generating mechanism in the anode. In addition, the
pore structure was also changing by dissolution of
the oxide phases inside the pores. Further changes
in the pore structure were generated by secondary
reaction (e.g., $3Ni^{+2} + NiFe_2O_4 \rightarrow 4NiO + 2Fe^{+3}$).
The oxygen evolution reaction also led to apparent
changes in the pore structure via gas bubble plugging
of the pores.

Besides being a non-static porous electrode, the
cermet anode is further complicated by two Faradaic
reactions, oxygen evolution and anodic nickel metal
dissolution. The oxygen evolution reaction occurs
primarily on the oxide phases of the cermet and
obtains its reactants chiefly from the electrolyte,
while the corrosion reaction is limited to the metal
phase and gets its reactants from the anode. The
exact microstructure of the anode varies from anode
to anode, making it complicated to determine even the
initial geometric accessibility of these phases to
the electrolyte.

Although the changing pore structure and multiple
Faradaic reactions are the most significant complica-
tions, other difficulties also exist. The electrical
conductivity of the oxide and metal phases are dif-
ferent by at least three orders of magnitude. This
electrode system consists of five phases: three
solid electrode phases, a liquid electrolyte phase,
and a gaseous product phase. The phase properties
are not clearly defined (e.g., the solubility of O_2
in cryolite is not well known).

Chizmadzhev and Chirkov (6) have discussed in
some depth porous electrodes more simple than this
cermet electrode. It is beyond the scope of this
paper to completely review their discussion, but
noting a few highlights of their paper is worthwhile.

The simple porous electrode has a fixed electrode
geometry and only one Faradaic process is occurring.
The ohmic drop in the matrix is fixed and negligible
compared to the electrolyte. The Faradaic process is
not coupled to any other chemical reactions and
occurs so fast that the rate is mass transport con-
trolled. Only two phases exist, the electrode matrix
and the electrolyte into which the reactants and
products of the Faradaic process are infinitely
soluble.

Since convection in the porous electrode matrix
is negligible, the flux of the component of interest
is the sum of two components, diffusion and migra-
tion. The driving force for the process is the
potential drop across the porous layer in a migration
controlled case and a concentration gradient in the
diffusion controlled case. The overall flux will be
influenced by the connected porosity of the matrix
and the tortuosity of the pores.

It was likely that the anodic dissolution process in the cermet electrode was influenced more strongly by the intrinsic characteristics of porous electrodes than by the parameters described earlier. Simple porous electrode theory was, therefore, used to guide further development of the material. Examination of the theory suggested the following steps could be taken to limit the anodic dissolution process.

Decrease porosity. This is difficult because the anodic dissolution process generates the pores. Freezing of electrolyte inside the pores by incorporating CaF_2 in the anode was tried. This failed because the CaF_2 slowly dissolved into the electrolyte but never reached a high enough concentration inside the pores to raise the liquidus temperature.

Increase tortuosity. This could be accomplished by incorporating a discontinuous metal phase inside the anode or by using more winding "metal worms" in the cermet.

Increase polarization for anodic dissolution. The thermodynamic polarization difference for Ni oxidation and oxygen evolution is the driving force for the anodic dissolution process. The potential drop across the porous layer is driven by the thermodynamic difference in polarization required for anodic dissolution of nickel (1.5 volts vs Al) and discharge of oxygen (2.2 volts vs Al). This difference can be decreased by using more noble and/or passivating metals.

Decrease temperature. Use of lower liquidus temperature electrolytes would decrease the anode temperature. Lowering of temperatures usually decreases the reaction rate of a chemical reaction.

Decrease active metal phase area. Use of a smaller percentage of metal would decrease the active area for anodic dissolution in the anode. Unfortunately, the electrical conductivity of the cermet also would decrease.

Development of an Improved Cermet

All of the above approaches were tried to some degree, but the greatest success was achieved by using an alternate metal phase.

An experimental screening of various pure metals and commercially available alloys was performed to find a metal or alloy that had a higher polarization requirement for anodic dissolution in the cryolite electrolyte than nickel. The metals were examined by performing a slow (1 mv/sec) linear sweep voltammogram, followed by a galvanostatic polarization at 1 amp/cm^2 for 1/2 hour. Corrosion currents and open circuit potentials obtained from the linear sweep voltammogram along with optical microscopic examination of the metal anodes were used to determine the corrosion resistance of the candidates being tested.

Table 1 summarizes the results of the metal and alloy screening program. None of the metals or alloys tested, except platinum, were sufficiently corrosion resistant to serve as an inert anode alone. However, copper and copper/nickel alloys were promising candidates for a metal phase in a $NiFe_2O_4$/NiO cermet. Copper is thermodynamically compatible with the preferred oxide phases ($NiFe_2O_4$/NiO). Copper

was also found to be dramatically more corrosion resistant than nickel in the metal screening program. Figure 7 shows linear sweep voltammograms obtained on both nickel and copper anodes. The hysteresis and absence of a break in the voltammogram for oxygen evolution when using a nickel electrode are good indications of an active corrosion process. Examination of the nickel electrode after removal from the electrolyte revealed a high degree of pitting corrosion and no adherent protecting film. On the other hand, copper displayed a limiting current behavior for the corrosion process and a break in the voltammetric curve for oxygen evolution. Since oxygen evolution is not thermodynamically preferred on a virgin metal surface, a passivating film between the copper metal and electrolyte must have been formed. Upon removal of the copper electrode, a thick adherent black film was found on the suface of the copper. Debye-Scherer X-ray diffraction identified the film to be 60-70% $CuAlO_2$ and 30-40% Cu_2O. The limiting current was the result of slow passage of ions through this passivating layer.

TABLE 1: ELECTROCHEMICAL CORROSION RESULTS OF METAL AND ALLOYS

METAL ALLOY	i_{corr} ma/cm^2	O.C.P. vs 2Al	COMMENTS
NICKEL	>1000	1.48	Massive pitting-corrosion; no adherent oxide layer
PLATINUM	<10	1.9	No observable corrosion
COPPER	123	1.87	Thick adherent oxide film
IRON	140	1.34	Thick film, spalling and pitting
TANTALUM	400	0.9	Massive corrosion
NICKEL (40) NIOBIUM (60)	>1000	0.9	Massive corrosion
MONEL 400	100	1.42	Microscopic pitting; preferential attack of Ni
INCONEL 600	168	1.58	Thin oxide layer with some spalling and internal voids
INCONEL X750	136	1.6	Very thin film; internal voids very little spalling
STAINLESS STEEL 316 (LOW CARBON)	500	1.1	Massive corrosion; spalling and pitting
HASTALLOY-C	80	1.3	Good oxide layer; no pitting
CABOT 214	190	1.6	Dense adherent oxide film; no spalling; internal voids

Copper alloys and platinum metal cermets in a $NiFe_2O_4$/NiO ceramic base were fabricated for comparison testing with the nickel metal cermet. The cermets were galvanostatically polarized for three

hours at 1 amp/cm2, after which slow linear sweep (1 mv/sec) voltammograms were obtained. Figure 8 shows the microprobe elemental dot map analysis of a cross-section of an area near the surface of the cermets after electrolysis.
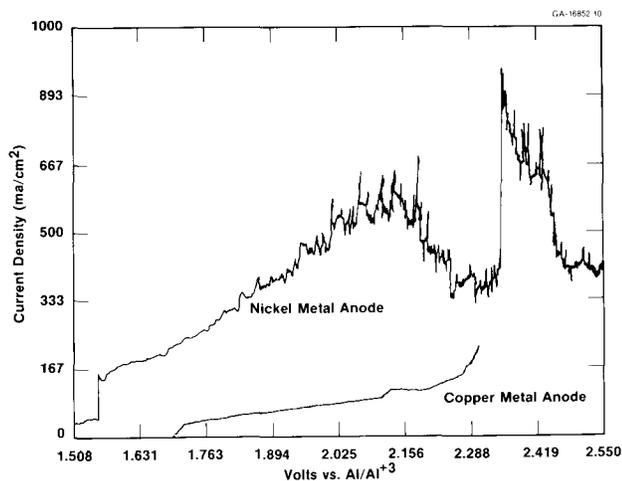

Figure 7. Voltammograms of Cu and Ni metal anodes.

Results of the anodic dissolution process in the nickel metal cermet are evident in the microprobe elemental dot maps. Internal penetration of electrolyte into the anode matrix is clearly shown by examining the Al, Na, F, and Ca elemental maps. The absence of any metal phase can be seen in the backscattered electron photograph (labeled SEM).

The platinum metal cermet (20% Pt) (also see Figure 8) displayed no internal penetration of electrolyte or loss of metal. The platinum cermet was unique in one other sense; grains of platinum were observed protruding from the electrode surface. Since the surfaces of all the cermets were polished to a mirror finish prior to electrolysis, the protruding grains of platinum were not the result of initial surface roughness. Chemically soluble oxide phases were selectively dissolving from the anode surface, leaving behind platinum grains. The platinum was lost from the anode matrix via grain fallout after the oxide phases surrounding the particle had dissolved. The high cost and low availability of noble metals (e.g., Pt) preclude their use in commercial inert anodes.

Figure 8 also shows typical microprobe results of some copper alloy cermets. The cermet containing 30 wt% alloy of a composition 90% nickel, 10% copper continued to show some internal penetration of electrolyte, but the amount was significantly decreased. A higher weight percentage copper cermet is also shown in Figure 8. Analysis of this cermet, containing 20 wt% alloy of composition 80% Cu:20% Ni, indicated no internal penetration of electrolyte. The micrographs also show metal was clearly present very close to the anode surface, but the nickel metal was selectively oxidized out of the copper alloy leaving behind essentially pure copper. The depth of this selective oxidation zone is less than 1 mm and was not observed to increase on extended electrolysis tests (up to 264 hours). In comparison, the nickel

cermet typically internally oxidizes altogether to a depth of approximately 0.5 mm in 3 hours.

Electrochemical results support the microprobe results. The comparison voltammetric results (displayed in a Tafel format) obtained on the $NiFe_2O_4/NiO-Ni$ alloy cermet and the $NiFe_2O_4/NiO-Cu$ alloy cermet are shown in Figure 9. After three hours of electrolysis, a corrosion current of approximately 30 ma/cm^2 was found on the Ni alloy cermet while the copper alloy cermet (80% Cu 20% Ni) showed no corrosion current down to the detection limits of the experiment (0.2 ma/cm^2).
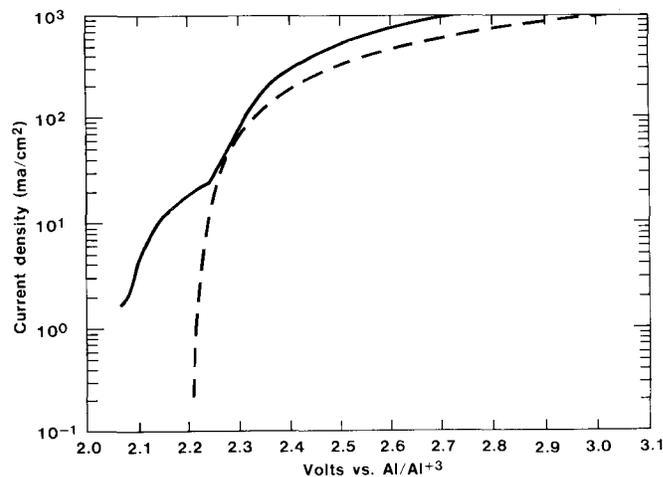

Figure 9. Comparison of voltammetric results for $NiFe_2O_4/NiO-Ni$ cermet and $NiFe_2O_4/NiO-Cu/Ni$ alloy cermet (——$NiFe_2O_4/NiO-Ni$ Cermet;---$NiFe_2O_4/NiO-Cu/Ni$ alloy cermet). (Results are displayed in a Tafel format and not I*R corrected.)

Parameters Affecting The Passivation

Clearly the elimination of the anodic dissolution process has been accomplished by switching from the nickel alloy phase in the $NiFe_2O_4/NiO$ anode. Passivation is dependent on the following three variables.

First, the anode matrix must be a cermet. The passivating oxide that forms has a tendency to spall off the surface of metal anodes during long-term electrolysis. The oxide phases of the cermet act as a mechanical barrier to spalling of the passivating layer.

Second, the alloy phase must be a copper rich copper-nickel alloy. Copper-nickel alloys of various compositions were incorporated into the $NiFe_2O_4/NiO$ ceramic base and tested using the above described experimental procedures. The anodes were found to be free of internal electrolyte penetration when the alloy was in the range of 40-95 wt% Cu, with the make-up being essentially Ni (see Figure 8 for two examples). The Ni is acting to cathodically protect the Cu metal in the cermet. Nickel is thermodynamically preferred to oxidize (1.5 volt vs Al) with respect to copper (1.8 volt vs Al). This preference leads to Ni being selectively oxidized from the metal phase. In the copper alloy cermet, all of the metal is not oxidized. The majority of metal (copper) is left unaltered, thus preventing electrolyte from entering the anode matrix. The manner in which the
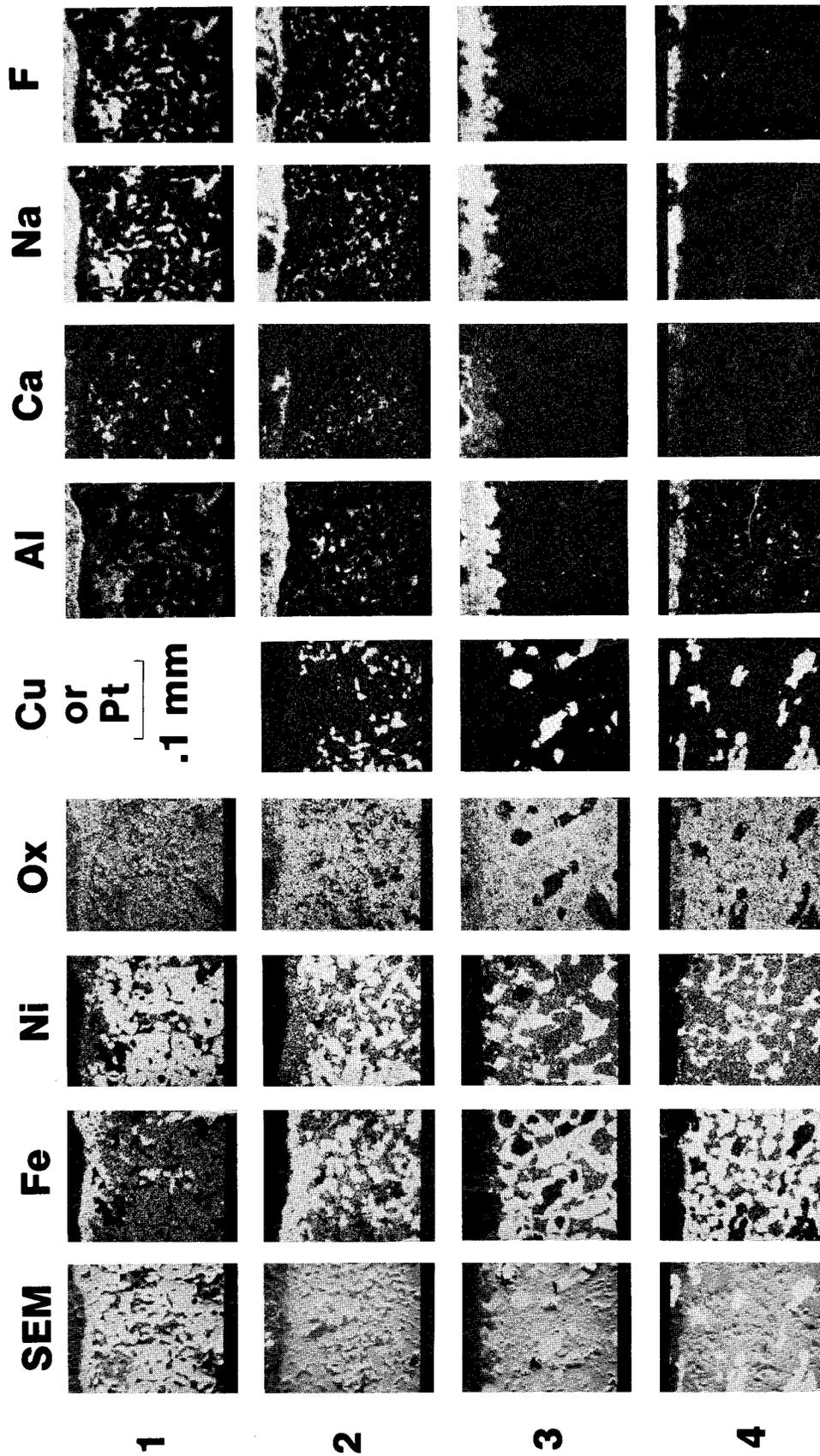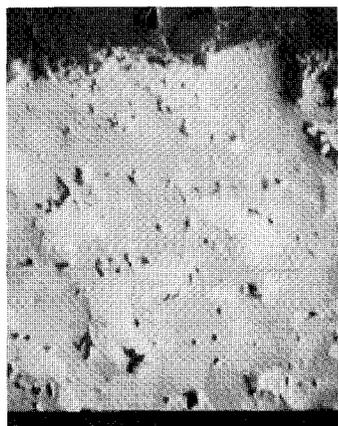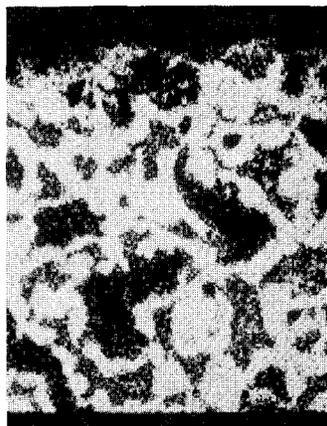
Figure 8. Microprobe comparison of various metal phases in $NiFe_2O_4/NiO-Ni$ cermets (1=$NiFe_2O_4$/NiO-Ni cermet, 2=$NiFe_2O_4$/NiO-Ni/Cu alloy cermet, 3=$NiFe_2O_4$/NiO-Cu/Ni alloy cermet, 4=$NiFe_2O_4$/NiO-Pt cermet).

SEM

Fe

Ni
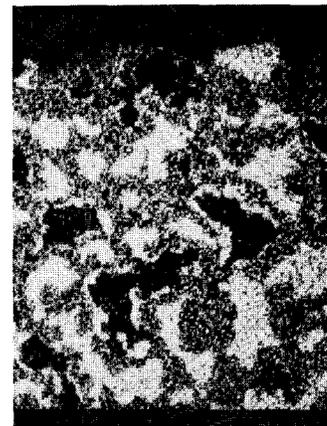
Ox
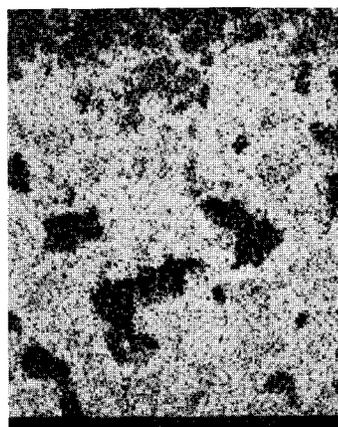
Cu
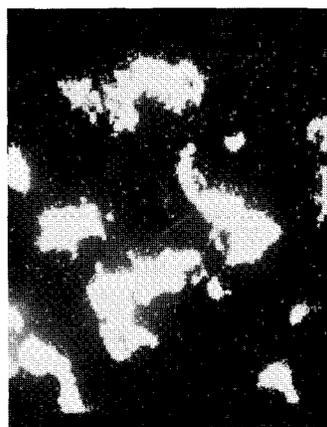
Al

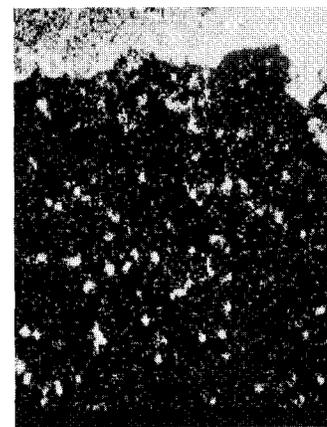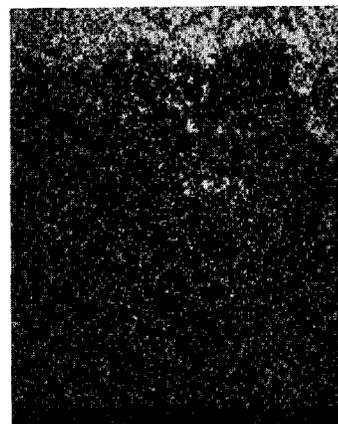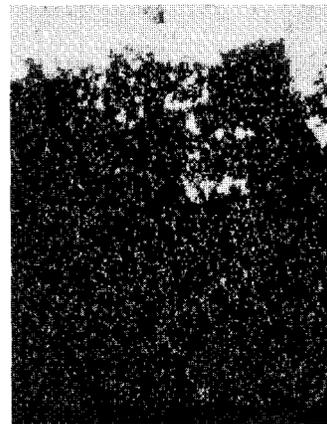# Ca

Na

F
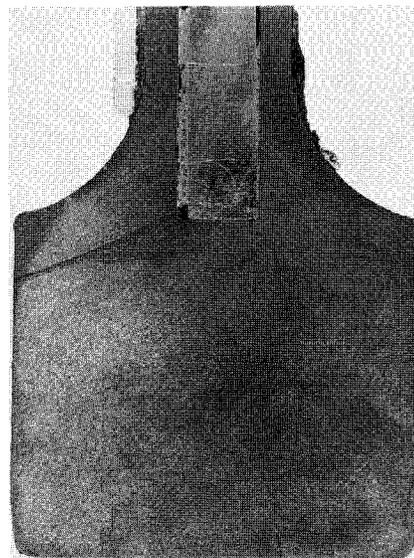
Figure 10. Internal penetration of electrolyte into $NiFe_2O_4/NiO-Cu/Ni$ alloy cermet with operation in a decreased Al_2O_3 concentration (63% saturation).

nickel oxidizes is also different in the copper alloy cermet. The nickel forms NiO inside the anode matrix instead of anodically dissolving into the electrolyte. The internal formation of NiO helps to plug pores, thus further blocking internal electrolyte penetration. Mass transport of the nickel cations in the copper alloy cermet is through a solid, whereas in the nickel alloy cermet mass transport was through the liquid electrolyte. Mass transport through a solid is generally much slower than through a liquid. As the nickel oxidation process continues, the diffusion path through the solid becomes longer, thus the process slows (probably parabolically) until the rate becomes equal to the chemical dissolution of the oxide phases in the anode.

The third requirement for passivation is a high concentration (activity) of Al_2O_3 in the electrolyte. Figure 10 shows the microprobe results of an 80% Cu-20% Ni alloy cermet after three hours of electrolysis in a decreased Al_2O_3 concentration electrolyte (Al_2O_3 = 63% of saturation). Internal penetration of electrolyte into the anode matrix was observed in microprobe results. It is encouraging that the degree of penetration was still less than the Ni metal cermet used in a saturated Al_2O_3 electrolyte (compare Figure 8 to Figure 10).

The dependence of the passivation of the cermet anode on Al_2O_3 concentration agrees with other results. As described earlier, Debye-Scherer X-ray diffraction identified the film on a copper metal anode to be approximately 60-70% $CuAlO_2$ and 30-40% CuO_2. Decreased Al_2O_3 in the electrolyte would decrease the ability to form the $CuAlO_2$ phase.
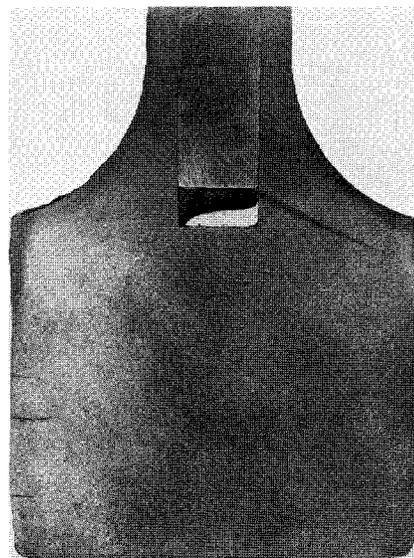

165 HRS. OF ELECTROLYSIS

11-B
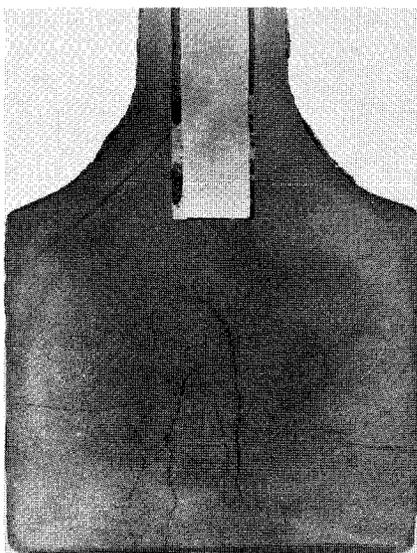
100 HRS. OF ELECTROLYSIS

11-A

264 HRS. OF ELECTROLYSIS

11-C

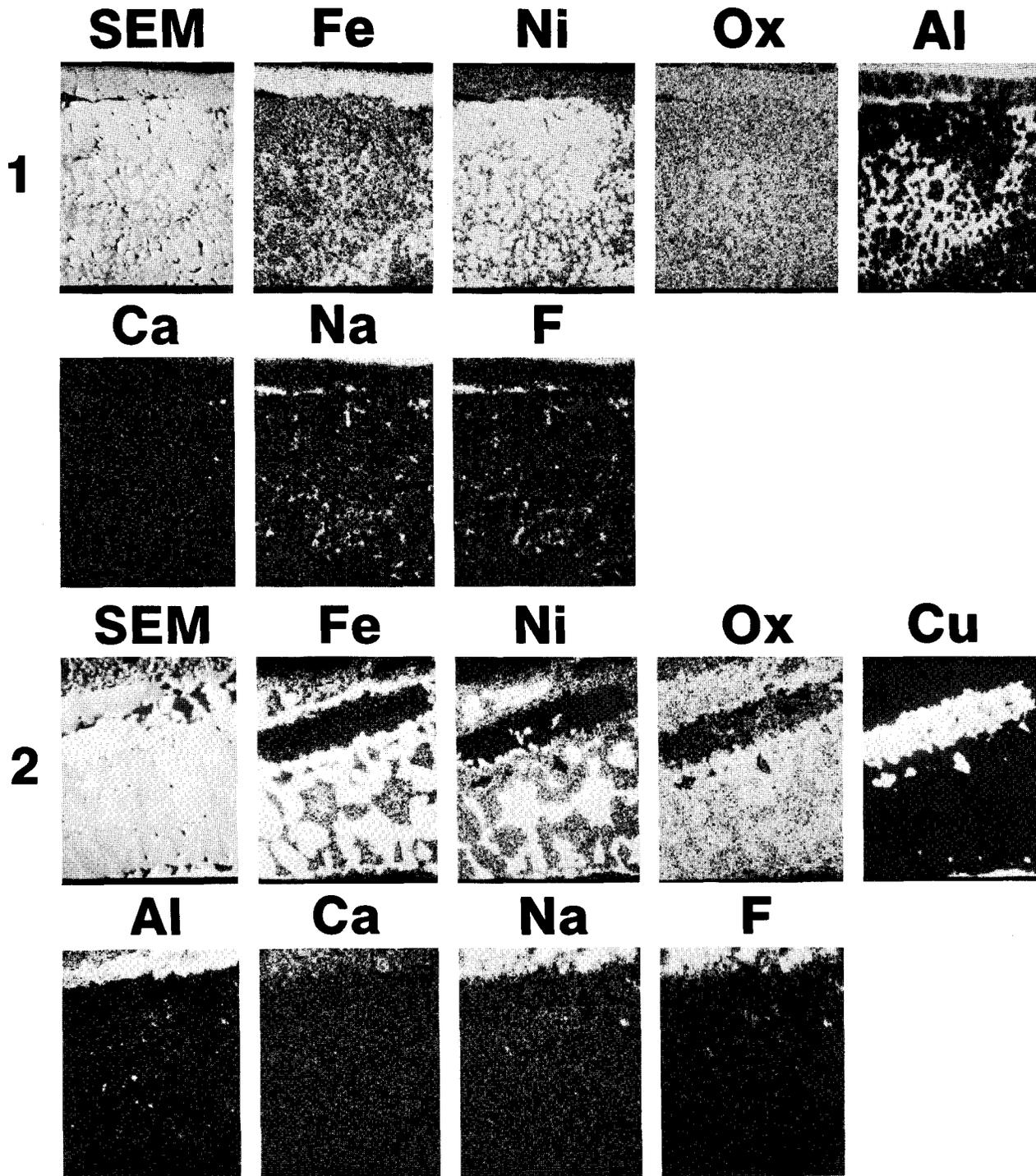Figure 11. Cross-sections of $NiFe_2O_4/NiO$-Cu/Ni alloy cermets.

Figure 12. Importance of metal phase composition and geometry on the internal penetration of electrolyte (1=NiFe$_2$O$_4$/NiO-Cu/Ni alloy cermet with alloy wires).

The copper alloy cermet anode was also found to be much more oxidation resistant when used in the saturated Al_2O_3 electrolytes than when used in air or oxygen at electrolysis temperatures. One copper alloy cermet was anodically polarized at 1 amp/cm^2 in a 1.15 NaF/AlF$_3$, 5% CaF$_2$, 7.5% Al_2O_3 electrolyte at 980°C for 30 hours. Another copper alloy cermet anode was placed in a furnace with an oxygen atmosphere at 980°C for 30 hours. On completion of 30 hours, both anodes were removed and examined for signs of internal metal oxidation. The electrolyzed anode had no signs of internal oxidation, whereas the cermet that was placed in the oxygen atmosphere had oxidized internally to a depth of approximately 2 mm. Since no dimensional loss of the electrolyzed anode was measurable, the anode was not internally oxidizing and then chemically dissolving at the same rate. (The dimensional loss of a copper cermet that was electrolyzed for almost 11 days was less than 1 mm.) The fact that the copper alloy cermet does not oxidize internally when used in the electrolyte can be explained by the passivating influence of the $CuAlO_2$ phase; the formation of which is dependent on Al_2O_3 being present in the electrolyte. Al_2O_3 can not participate in a passivating film during an O_2 atmosphere oxidation of the material.

Parameters Not Influencing The Passivation

The passivation was found to be independent of electrolysis time, current density, percentage of the alloy in cermet, microstructural size of the alloy grains, and dissolved metal in the electrolyte. Figure 11 shows photographs of cross-sectioned anodes after 100 hours (11-A), 165 hours (11-B) and 264 hours (11-C) of electrolysis. No zone of internal oxidation is visible in any of the anodes. A nickel alloy cermet internally oxidizes to a depth of 1 cm in 100 hours (see Figure 3), 1.5 cm in 165 hours, and 4.0 cm in 264 hours. The internal depth to which the alloy phase became enriched in copper was also shown to have been limited to less than 0.1 mm in all of the above anodes tested. These extended time electrolysis tests of the copper alloy cermet show that the passivation is independent of time.

The effect of current density was tested by performing galvanostatic polarizations at three times the normal commercial current density (3 amps/cm^2) for three hours. Linear sweep voltammograms were then performed on the anode. After the electrolysis period, the anode was cross-sectioned and examined by microprobe analysis as described previously. No corrosion currents were observed during the voltammetric scan, and no internal penetration of electrolyte was observed with the microprobe analysis. Current densities higher than 3 amps/cm^2 were not tested.

Passivation was independent of the weight percentage of the alloy in the cermet. Cermets containing 5%, 10%, 15%, 17% and 20% metal were fabricated and tested as was previously described. None of these compositions showed any corrosion current or internal penetration of electrolyte into the anode matrix structure. Cermets containing higher percentages of metal did not produce anodes of sufficient quality to test. High percentages of metal coupled with high sintering temperatures caused the anodes to either melt, bleed out the metal phase, or exhibit laminar cracks during the fabrication process. Recent experiments have shown that the metal content can be increased by lowering the sintering temperature and/or increasing the nickel content of the copper alloy. Corrosion testing of these increased metal content cermets has not yet been completed.

The Ni cermet had a high conductivity (300 ohm^{-1} cm^{-1}) due to the reaction sintering process producing continuous metal worms that wind throughout the cermet. On the other hand, the copper cermet had an acceptable but lower conductivity (90 ohm^{-1} cm^{-1}) because the metal phase was distributed as individual particles in the ceramic phase. A nickel cermet was fabricated with individual nickel particles similar to the copper cermet. The individual nickel particle cermet was tested with a three-hour galvanostatic polarization and subsequent microprobe analysis. The microprobe analysis (see Figure 12) indicated internal penetration of electrolyte and loss of metal. This proved that passivation of the metal was due to the use of copper alloys, not isolation of the metal grains. Since a continuous metal phase in the cermet gave such high conductivity, there was interest in trying to obtain a continuous metal phase in the copper alloy cermet. A concern existed that a more accessible continuous copper phase might also be prone to anodic dissolution. A copper alloy cermet was fabricated using wires (30μm x 100μm x 3000-5000μm) as the metal phase. The purpose was to simulate a continuous metal phase exposed to the electrolyte in the copper alloy cermet. The copper wire cermet electrode was tested in a similar manner to the previous cermets. No corrosion current was observed on the cermet. Figure 12 shows the microprobe results. No significant internal penetration of electrolyte was observed along the copper wire even though the wire was more electrochemically accessible than the reaction sintered nickel metal cermet (nickle metal worms had a diameter of approximately 10μm). This result indicates that the use of the copper alloy, not the microstructural arrangement of the alloy, was the important passivation parameter in the copper cermet anode. A continuous wormy copper metal phase has not yet been achieved, but a very conductive, corrosion resistant anode may be possible if a method can be found to produce such an anode.

Dissolved aluminum metal does not have an effect on the passivation. The anodes shown in Figure 11 were electrolyzed in a cell (see Figure 2) that had an aluminum cathode. Experiments were also performed in the three-hour electrolysis cell (see Figure 1) with an aluminum cathode. In this cell the cathode area to anode area is much greater than in commercial cells. In commercial cells the ratio of cathode area to anode area is in the range of 1.6-1.2 while in the three-hour experimental cell the ratio was approximately 200. This large excess of cathode area insured a dissolved metal content in the electrolyte even though oxidizing components (NiO, Fe$_2$O$_3$, and Cu$_2$O) were dissolving into the electrolyte from the anode.

CONCLUSION

This study has demonstrated that a practical and stable metal phase in an oxygen producing anode used for aluminum smelting is achievable. Nickel was an unacceptable metal phase in a cermet anode because of the tendency to anodically dissolve. A stable metal phase was developed by using a copper rich copper-

nickel alloy in a $NiFe_2O_4/NiO$ ceramic base. Since this metal phase did not use expensive and rare noble metals it shows practical commercial promise. The stability of the metal phase has been shown to be dependent on three factors: (1) use of a cermet to provide a mechanical barrier to spalling; (2) use of copper rich copper-nickel alloys to cathodically protect the copper metal during the initial phase of electrolysis; and (3) high Al_2O_3 concentration (activity) in the electrolyte to assure the formation of a passivating $CuAlO_2$.

This study has also shown an experimental approach for screening metal and/or alloys (either independently or incorporated into cermets) that should be generally applicable to other candidate materials being considered as inert anodes for aluminum smelting. The experimental approach uses slow scan linear sweep voltammetry, galvanostatic polarizations, and microprobe elemental dot map analysis to examine the resistance of metal and alloys to anodic dissolution in cryolite-base melts. The important experimentally determined variables are the corrosion current and the open circuit potential as determined from the voltammetry, and the degree of electrolyte penetration is determined with microprobe elemental dot map analysis.

ACKNOWLEDGEMENT

REFERENCES

1. K. Grjotheim, et al., Aluminium Electrolysis (Dusseldorf FRG:Aluminium-Verlag, 1982) 261-265; 405-411; K. Horinouchi, N. Tachikawa, K. Yamada, "DSA in Aluminum Reduction Cells" (Paper presented at the First International Symposium on Molten Salt Chemistry and Technology, Kyoto Japan, April 20-22) B-209.

2. Siba Ray, U.S. Patent 4455211.

3. Digby D. Macdonald, Transient Techniques in Electrochemistry (New York, New York, Plenum Press, 1977) 17-19.

4. K. Grjotheim, et al., Aluminium Electrolysis (Dusseldorf FRG:Aluminium-Verlag, 1982) 202-205.

5. D. H. DeYoung, "Solubility of Oxides for Inert Anodes in Cryolite-Based Melts" (paper to be presented at 1986 AIME meeting in New Orleans).

6. Yu. A. Chizmadzhev and Yu. G. Chirkov, Chapter 5,"Porous Electrodes," COMPREHENSIVE TREATISE ON ELECTROCHEMISTRY, Vol. 6; Electrodics; Transport; edited by E. Yeager, et al, (New York, N.Y. 1983) 317-391.